## SHORT COMMUNICATION

## Differential Colonization of the Plant Vasculature **Between Endophytic Versus Pathogenic** Fusarium oxysporum Strains

Domingo Martínez-Soto, Houlin Yu, Kelly S. Allen, and Li-Jun Ma<sup>†</sup>

Department of Biochemistry and Molecular Biology and the Plant Biology Graduate Program, University of Massachusetts, Amherst, MA 01003, U.S.A.

Accepted for publication 22 October 2022.

Plant xylem colonization is the hallmark of vascular wilt diseases caused by phytopathogens within the Fusarium oxysporum species complex. Recently, xylem colonization has also been reported among endophytic F. oxysporum strains, resulting in some uncertainty. This study compares xylem colonization processes by pathogenic versus endophytic strains in Arabidopsis thaliana and Solanum lycopersicum, using Arabidopsis pathogen Fo5176, tomato pathogen Fol4287, and the endophyte Fo47, which can colonize both plant hosts. We observed that all strains were able to advance from epidermis to endodermis within 3 days postinoculation (dpi) and reached the root xylem at 4 dpi. However, this shared progression was restricted to lateral roots and the elongation zone of the primary root. Only pathogens reached the xylem above the primary-root maturation zone (PMZ). Related to the distinct colonization patterns, we also observed stronger induction of callose at the PMZ and lignin deposition at primary-lateral root junctions by the endophyte in both plants. This observation was further supported by stronger induction of Arabidopsis genes involved in callose and lignin biosynthesis during the endophytic colonization (Fo47) compared with the pathogenic interaction (Fo5176). Moreover, both pathogens encode more plant cell wall-degrading enzymes than the endophyte Fo47. Therefore, observed differences in callose and lignin deposition could be the combination of host production and the subsequent fungal degradation. In summary, this study demonstrates spatial differences between endophytic and pathogenic colonization, strongly suggesting that further in-

<sup>†</sup>Corresponding author: L.-J. Ma; lijun@biochem.umass.edu

Funding: This project was supported by Natural Science Foundation (IOS-165241) and the United States Department of Agriculture (USDA) National Institute of Food and Agriculture (NIFA) (MAS00496). L.-J. Ma is also supported by an Investigator Award in Infectious Diseases and Pathogenesis by the Burroughs Wellcome Fund BWF-1014893 and the National Eye Institute of the National Institutes of Health under award number R01EY030150. H. Yu is also supported by a Lotta M. Crabtree Fellowship and Constantine J. Gilgut Fellowship. K. S. Allen is also supported by USDA/SCRI/NIFA award (2016-68004-24931). The funding bodies played no role in the design of the study and collection, analysis, and interpretation of data and in writing of the manuscript.

*e*-Xtra: Supplementary material is available online.

The author(s) declare no conflict of interest.



Copyright © 2023 The Author(s). This is an open and distributed under the CC BY-NC-ND 4.0 International license. Copyright @ 2023 The Author(s). This is an open access article

vestigations of molecular arm-races are needed to understand how plants differentiate friend from foe.

Keywords: differential plant colonization, endophytic fungus, Fusarium oxysporum Fo47, pathogenic fungus, plant-fungus interaction

The ascomycete fungal Fusarium oxysporum species complex (FOSC) includes plant pathogens that are responsible for devastating vascular wilt diseases of many economically important crops, including tomato (Michielse and Rep 2009), cotton (Halpern et al. 2018), watermelon (Rahman et al. 2021), and banana (Viljoen et al. 2020). Causing billions of dollars in annual yield losses, F. oxysporum is listed among the top five most important plant pathogens with direct impacts on the global economy and food security (Dean et al. 2012). Typical vascular wilt symptoms include stunting, leaf epinasty, chlorosis, necrosis, and vascular bundle discoloration, all resulting from the colonization of the plant vascular xylem tissue by this group of pathogens (Lagopodi et al. 2002; Li et al. 2017; Olivain et al. 2003, 2006). It is well-documented that hostspecific vascular colonization is controlled by host-specific mobile accessory chromosomes (Armitage et al. 2018; Delulio et al. 2018; Dong et al. 2015; Fokkens et al. 2020; Galazka and Freitag 2014; Hane et al. 2011; Ma et al. 2010, 2013; van Dam et al. 2016; Vlaardingerbroek et al. 2016; Wang et al. 2020; Williams et al. 2016; Yang et al. 2020; Yu et al. 2020; Zhang and Ma 2017). Effector genes encoded in these accessory chromosomes can interfere with plant defense and assist the pathogen propagation (Houterman et al. 2007; Ma et al. 2010; Rep et al. 2004; Yang et al. 2020).

Arguably, nonpathogenic F. oxysporum strains are more prevalent in nature, including many endophytes associated with land plants (Bao et al. 2004; Demers et al. 2015), offering protective advantages to host plants that are exposed to diverse environmental stresses (Kistler 1997; Ma et al. 2013; Michielse and Rep 2009). Notably, some endophytic F. oxysporum strains have been used to suppress Fusarium wilts (Alabouvette 1986). For instance, F. oxysporum Fo47, one of several nonpathogenic strains isolated from the Châteaurenard region disease-suppressive soil, has been used to control Fusarium diseases in different crops, including cucumber, carnations, dianthus, tomato, and the model plant Arabidopsis (Brader et al. 2017; de Lamo and Takken 2020; Guo et al. 2021). The same strain is also reported to contribute systemic induced resistance in pepper and tomato plants (Aimé et al. 2013; Veloso and Díaz 2012).

Phenotypically, pathogens lead to diseased plants, while endophytic plant interactions result in healthy plants. At the transcription level, our recent study revealed a shared pattern of expression for about 80% of plant genes when *Arabidopsis* was independently challenged with the endophyte Fo47 or the pathogen Fo5176 (Guo et al. 2021). The remaining approximately 20% of differentially expressed genes offered insight into these two distinct interactions. Within 12 h postinoculation, the pathogenic interaction activated plant stress responses and suppressed plant growth and development-related functions, while the endophytic interaction mainly attenuated host immunity and activated plant nitrogen assimilation (Guo et al. 2021).

The conventional wisdom is that only pathogenic FOSC strains, not endophytes, can colonize plant vascular xylem tissue, a hallmark of vascular wilt diseases. This was supported by electron microscopic study of the endophyte Fo47, which was able to grow at the host root surface and colonize epidermal and cortical cells but was deterred from entering the plant vascular tissue (Benhamou and Garand 2001; Benhamou et al. 2002). In recent years, this conventional wisdom was challenged by multiple observations. For example, in addition to inducing a priming effect (significant expression of genes involved in plant defense), the endophyte strain *F. oxysporum* CS-20 was observed in the xylem of cucumber seedlings (Pu et al. 2014). Moreover, Fo47 was reported to colonize tomato xylem under both confocal and electron microscopy (Redkar et al. 2022).

Upon learning that endophytic F. oxysporum strains may occupy plant vasculature, the question of how pathogenic and endophytic interactions differ emerges as a key unknown entity in the field of plant-microbe interactions. This study addresses this question by tracking the endophyte and pathogen colonization processes over 16 days postinoculation (dpi) in two hosts, Arabidopsis thaliana Columbia-0 and tomato Solanum lycopersicum ev. M82. The endophytic strain F. oxysporum Fo47 that can colonize both plant hosts, the Arabidopsis pathogenic strain Fo5176, and the tomato pathogenic strain Fol4287 were used for the study. Interestingly, fungal hyphae from Fo47 were observed in the vasculature of both Arabidopsis and tomato roots. But such presence was limited to the vasculature of lateral roots and elongation zone of primary roots. We revealed the most significant difference at the primary-root mature zone (PMZ), as the endophyte was excluded from the vasculature of that zone in both host plants but both pathogens were present in the vasculature of that root zone. We also observed stronger callose and lignin deposition at the PMZ and at the junctions of the primary and the lateral roots along with the exclusion of endophyte from the PMZ.

The endophytic strain Fo47 and two pathogenic strains (Fo5176 and Fol4287) were inoculated into two plant hosts according to published inoculation protocols with some modifications (Di Pietro and Roncero 1998; Guo et al. 2021). To briefly describe the experiment, cleaned *Arabidopsis* and tomato roots were soaked in 10<sup>6</sup>-spores/ml suspensions for 45 min. Inoculated plants were then gently transplanted in sterilized soil (discussed below). In agreement with existing knowledge, Fo47-inoculated plants remained healthy (Fig. 1A and I), while Fo5176- and Fol4287-infected plants developed disease symptoms at 6 and 12 dpi respectively (Fig. 1E and M). The process of fungal colonization of the plant root was tracked daily, using confocal microscopy after WGA-Alexa Fluor staining of fungal cell walls and propidium iodide staining of plant cell walls (Ghareeb et al. 2011).

Following the progression of the endophyte Fo47 in *Arabidopsis* lateral roots, we repeatedly observed the same process. At 1 dpi and after the germination of microconidia around 6 hpi, Fo47 hyphae were growing on the *Arabidopsis* root surface and penetrating root epidermis cell layers (Fig. 1B). Between 2 and 3 dpi, Fo47 continued to colonize the root cortex (Fig. 1C). At 4 dpi, Fo47 reached the lateral root vascular system (protoxylem

and metaxylem) (Fig. 1D). The *Arabidopsis* pathogenic strain Fo5176 followed temporal and spatial patterns similar to the fungus growing through the epidermal cells, eventually reaching the root vascular system at 4 dpi (Fig. 1F to H).

A similar course of colonization was observed for the endophyte Fo47 in colonizing tomato plants and reaching the vasculature of lateral roots. At 1 dpi, Fo47 penetrated the tomato epidermal tissue (Fig. 1J), and it then colonized the root cortex at 2 and 3 dpi (Fig. 1K). The root vascular system of lateral roots was colonized at 4 dpi (Fig. 1L). Analogous times of colonization were registered for Fol4287 (Fig. 1N to P). The fungus penetrated the epidermis, then the cortex and reached into vessel elements at 4 dpi (Fig. 1P). We also observed that Fo47 reached the vessel cells of the elongation zone of the primary roots just before the presence of lateral roots (Supplementary Fig. S1).

We further confirmed the colonization of the endophyte Fo47 in the root vasculature of *Arabidopsis* and tomato plants by amplifying and sequencing Fo47 strain-specific effector genes, namely, FOZG\_17267 (jgi|FusoxFo47\_2|262755), FOZG\_10369 (jgi|FusoxFo47\_2|239495), and FOZG\_17668 (jgi|FusoxFo47\_2|276745) (Supplementary Fig. S2), and by tracking the Fo47 strain tagged with red florescent protein (Fo47-RFP [Supplementary Fig. S3]).

With the confirmation of the presence of endophyte Fo47 in the vascular vessels of the lateral roots of both plant hosts, we examined fungal-plant interactions along primary roots in both plant hosts. A similar fungal progression as described above for the lateral roots was also observed at the elongation zone of primary roots for both endophytic and pathogenic strains in both plant hosts. Interestingly, distinct colonization patterns between the endophyte and both pathogens became apparent once we moved our focus to the PMZ, where the protoxylem vessels are specified and lateral roots are clearly visible (Cajero-Sánchez et al. 2017; Kondo et al. 2014; Somssich et al. 2016). While the pathogenic strains reached the vessel elements of Arabidopsis (Fig. 2A) and tomato (Fig. 2C) plants, the endophyte Fo47 was absent from the vascular vessels from the PMZ in both Arabidopsis (Fig. 2B) and tomato plants (Fig. 2D). Another important difference was the first-time observation of chlamydospores in the lateral roots of both Arabidopsis and tomato plants colonized by the endophyte Fo47 at 5 dpi (Fig. 2F and H), as chlamydospores production had only been described in the later infection stages by pathogens (Akhter et al. 2016; Cal et al. 1997; Gordon 2017).

Inspecting stems above the ground, we observed the presence of only pathogenic strains in the vasculature tissues, not the endophytic strain Fo47, in both plant hosts (Fig. 3A), which is consistent with the difference observed in the PMZ. We further monitored fungal presence in the above-ground plant tissues using quantitatve PCR (qPCR). Total DNA was extracted from the stems of inoculated plants. The F. oxysporum actin gene was used to detect fungal strains. Using the A. thaliana pentatricopeptide repeat gene as the reference, we detected the relative abundance of the A. thaliana pathogen Fo5176, the endophyte Fo47, and the mock-inoculated samples in the Arabidopsis stems to be 0.7, 0.0, and 0.0, on average, respectively (Fig. 3B). Similarly, using tomato beta-tubulin gene as the reference, we detected the relative abundance of the tomato pathogen Fol4287, the endophyte Fo47, and the mock-inoculated samples to be 1.1, 0.0 and 0.0 respectively (Fig. 3C). With no difference between the stems of mock-inoculated and the Fo47-inoculated plants provided us strong evidence that the endophyte wasn't able to advance to plant above-ground tissues. The exclusion of endophytic Fo47 in the PMZ likely contributes to the absence of endophytic F. oxysporum in the plant stems, as reported in literature (de Lamo and Takken 2020).

To address whether a plant responds differently to an endophyte versus a pathogen, we examined the plant cell-wall composition, focusing on callose, lignin, and suberin. Callose is a high molecular weight polymer comprised of beta-(1,3)-glucans, documented to accumulate at sites of pathogen attack (Iriti and Faoro 2009) that can be measured using the aniline blue staining method (Zhang et al. 2015). Similarly, lignin is an important component of cell walls of vascular plants, considered a first line of defense against pathogenic fungi (Bhuiyan et al. 2009; Lee et al. 2019). Suberin is a lipophilic macromolecule produced in the plant cell walls when protection and insulation toward the surroundings is needed (Graca 2015). We visualized lignin with basic fuchsin and suberin with auramine O (according to the methodologies described by Kurihara et al. 2015 [details below]).

Significantly, we observed stronger induction of callose at the PMZ (Fig. 4A to H) and lignin at junctions of primary and lateral roots by the endophyte (Fig. 4I to P) in both *Arabidopsis* and tomato roots colonized by the endophyte Fo47, as compared with either pathogen-inoculated or mock-inoculated plants. However, no visible differences in suberin deposition were observed (Supplementary Fig. S4).

To quantify the callose induction, we measured the relative intensity of aniline blue. At 3 dpi, *Arabidopsis* plants colonized by Fo47 showed 1.5 times greater intensities than mock-infected plants (*P* value of 8.8E-7) and plants infected with pathogenic strain Fo5176 (*P* value of 7.5E-7) (Fig. 4D). Similarly, the tomato plants colonized by Fo47 showed 6.9 and 2.6 times greater

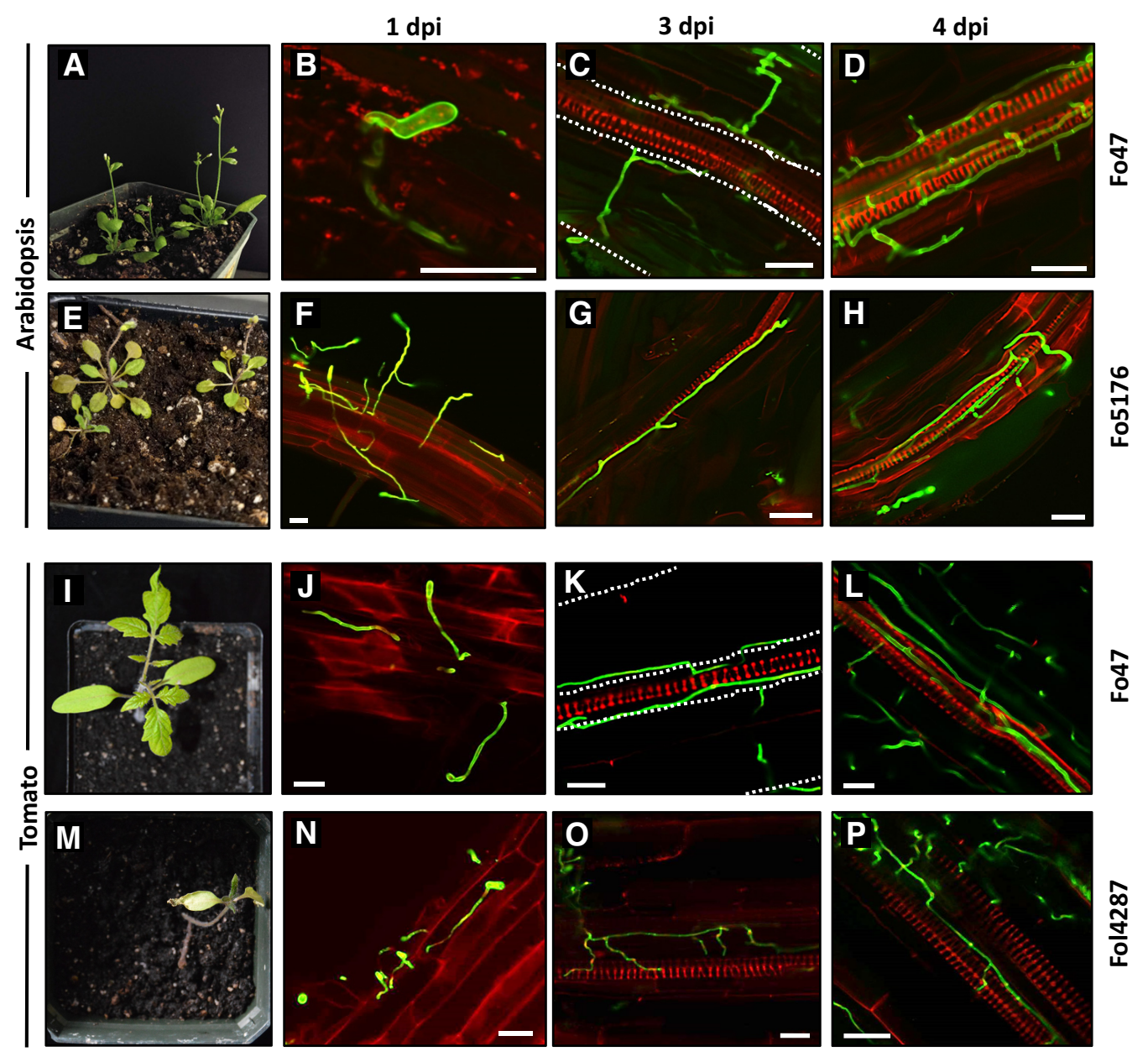


Fig. 1. The course of lateral root colonization by *Fusarium oxysporum* strains. In all microscopy photographs, fungal structures are shown in green and plant root tissues in red. **A to D**, *Arabidopsis* plants and roots colonized by Fo47. **E to H**, *Arabidopsis* plants and roots infected by Fo5176. **I to L**, Tomato plants and roots colonized by Fo47. **M to P**, Tomato plants and roots colonized by Fo47 (without symptoms) or infected by Fo5176 (with symptoms), respectively, at 16 days postinoculation (dpi). Images in I and M show representative tomato plants colonized by Fo47 (without symptoms) or infected by Fo14287 (with symptoms), respectively, at 12 dpi. Images in B, F, J, and N show root tissue penetration by the "penetration hyphae" or "appressorium-like small structure". Images in C, G, K, and O show *Fusarium* strains growing close to vessels cells. White dotted lines in C and K indicate the root cortex zone. Images in D and L show Fo47 has reached the root protoxylem and metaxylem of lateral roots. Images in H and P show Fo5176 and Fo14287 have reached the vessels cells of primary roots. Scale bar = 20 μm.

intensities than mock-infected plants (*P* value of 5.7E-7) and plants infected with pathogenic strain Fol4287 (*P* value of 1.9E-5), respectively (Fig. 4H). Notice, callose deposition was observed only in vessel elements and around vascular cells (Fig. 4A and E).

The measurement of relative intensity of fuchsin revealed the induction of lignin deposition at early stages in roots of both plant hosts colonized by the endophyte. For instance, Fo47 colonization *Arabidopsis* plant exhibited 1.3 times greater and 1.5 times greater intensities compared with mock-infected plants (*P* value of 5.2E-6) and plants infected with pathogenic strain Fo5176 (*P* value of 9.5E-6) (Fig. 4L). Our observations were similar in tomato plants, where Fo47 colonized plants produced 2.5 and 2.4 more than mock-infected tomato plants (*P* value of 0.0012) and Fol4287 infected plants (*P* value of 0.0011), respectively (Fig. 4P). The lignin deposition was observed at the junctions of the primary and the lateral roots (Fig. 4I and M).

To understand potential mechanisms underpinning the differential induction of callose and lignin in plants colonized by the endophyte Fo47 and the pathogen Fo5176, we analyzed our former published metatranscriptomic data to examine the expression of Arabidopsis genes involved in callose biosynthesis (GLUCAN SYNTHASE-LIKE [GSL]) (Ellinger and Voigt 2014) and key regulators of the lignin biosynthetic pathways (MYB46, MYB63, and KNAT) (Liu et al. 2018; Vanholme et al. 2010). Nine of the 12 GSLs were up-regulated when inoculated with the endophyte Fo47 when compared with the pathogen at 4 dpi (Supplementary Fig. S5A). Among the three key lignin biosynthesis genes (Supplementary Fig. S5B), MYB46 and KNAT show pronounced downregulation by the pathogen at 12 and at 96 hpi, respectively, while MYB63 was continuously up-regulated only in the endophytic interaction through the full course of interaction. The unique induction by the endophyte is consistent with our observation that Fo47 induces stronger callose and lignin deposition (Fig. 4A, E, D, and H).

The difference in plant cell-wall composition can also be attributed to the differences in degradation of the plant cell wall by the fungus. In fact, both pathogens, Fo5176 and Fol4287, encode higher numbers of cell wall-degrading enzymes, including enzymes lacking homologs in Fo47 (Supplementary Table S1; Supplementary Fig. S6A). For example, the genome of Fo47 only encodes one glycoside hydrolase, while Fol4287 and Fo5176 genomes contain 13 and nine glycoside hydrolases, respectively. A total of 20 enzymes in Fo5176 did not have ortholog pairs in Fo47 and showed clear upregulation during plant infection at one or multiple timepoints postinoculation (Supplementary Fig. S6C, asterisks). The exclusion of endophytic Fo47 from aboveground plant tissues and these comparative genomics results, suggest that pathogenic F. oxysproum has an improved capacity to degrade host structural structures to facilitate colonization. Alternatively, these plant structural defenses are either not triggered or actively suppressed by the pathogenic isolates.

This study documented the presence of the endophytic *F. oxysporum* Fo47 strain in the xylem of lateral roots and the elongation zone of the primary root in both *Arabidopsis* and tomato plants, in agreement with recent literature reports (Pu et al. 2014; Redkar et al. 2022). However, this work also demonstrated under microscopy and with the quantification of the relative fungal biomass that, in contrast to *F. oxysporum* pathogenic strains Fo5176 and Fol4287, the endophytic strain was excluded from the vasculture xylem of the PMZ and the stem plant tissues in the two most important host models for studying the interaction of *F. oxysporum* with plants. This confirms previous reports on the restricted endophytic fungal growth to the outermost cell layers of host plants (Benhamou and Garand 2001; Benhamou et al. 2002, Pu et al. 2014). Instead of the uncertainty

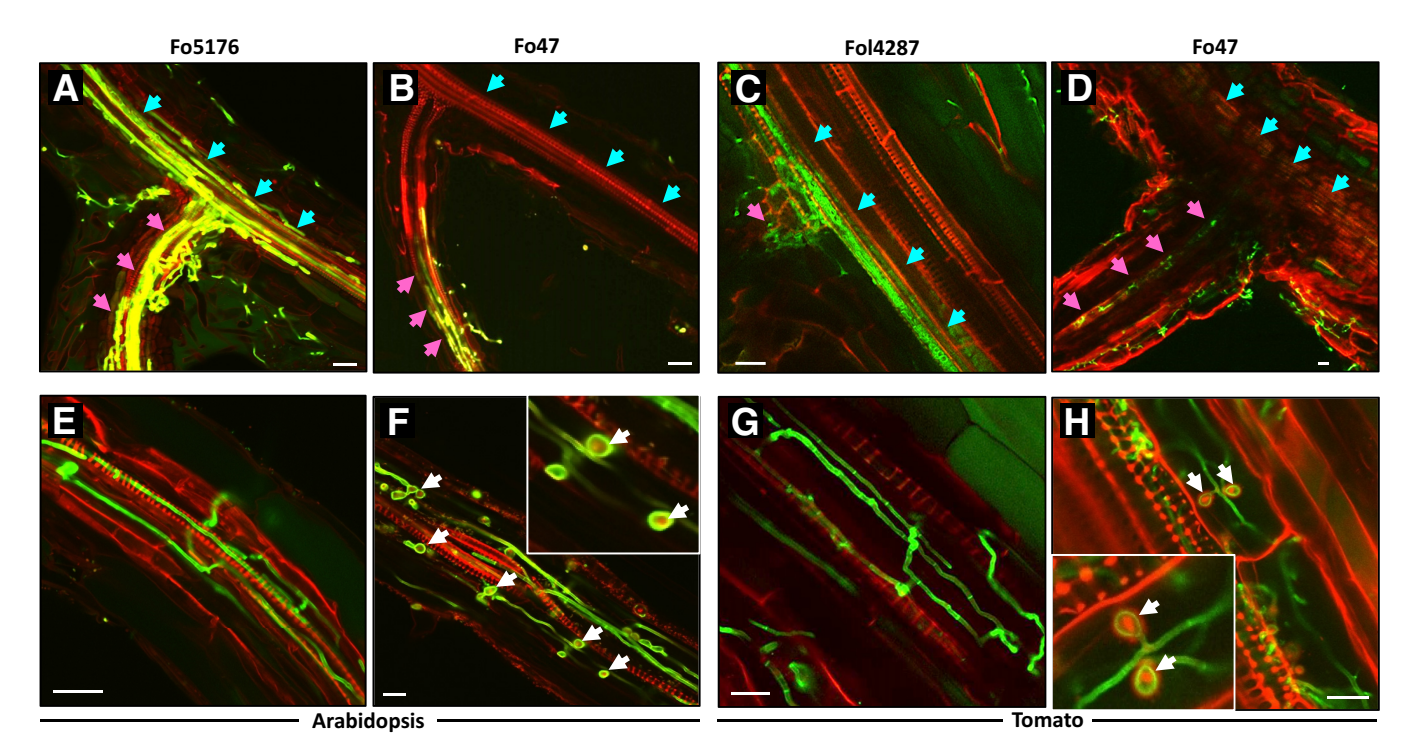


Fig. 2. Differences in colonizing primary root above maturation zone by endophyte Fo47 and pathogenic strains and early chlamydospore production of Fo47 in lateral roots. Fungal structures are shown in green and plant root tissues in red. **A and B,** *Arabidopsis* roots colonized by Fo5176 and Fo47, respectively. **C** and **D,** Tomato roots colonized by Fo14287 and Fo47, respectively. Images in B and D show Fo47 reaching vessel cells of lateral roots (pink arrows) but not the primary root (blue arrows), in contrast to pathogenic strains Fo5176 (A) and Fo14287 (C), which reach both lateral (pink arrows) and primary roots (blue arrows). **E to H,** The production of chlamydospores of Fo47 (white arrows) in lateral roots of *Arabidopsis* (F) and tomato (H) begins to be observed after 5 or 6 days postinoculation. Notice the absence of Fo5176 and Fo14287 spores (E and G, respectively) in roots of *Arabidopsis* and tomato, at the same time frame. Scale bar =  $20 \mu m$ .

about whether endophytic isolates can colonize plant xylem, this study unites these two different views based on the spatial occupation of the endophyte within the host plants.

In connection to this pronounced difference that distinguishes the endophyte from both pathogens, we observed significant callose deposition in the primary root and lignin deposition at the junctions of primary root and lateral roots upon endophyte colonization. Both callose and lignin are often rapidly deposited at sites of pathogen infection and in response to injuries (Hückelhoven 2007). Depositions of amorphous granular material, as well as lignification into pit membranes, have been suggested to contribute to plant defense against or preventing plant cellwall degradation (Araujo et al. 2014). Redkar et al. (2022), Bishop and Cooper (1983), and Pegg 1976 reported the deposition of amorphous granular material around the endophyte Fo47 hypha. While this is likely not the only factor that differentiates the endophytic and pathogenic interactions, callose and lignin deposition are certainly involved in constraining the endophyte spread from lateral root vasculature to the primary root maturation zone.

The observed differences of plant cell-wall components could result from the interactions between host production and subsequent degradation by the fungus. From the host perspective, we observed the induction of genes involved in biosynthesis pathways at the transcriptional level. From the fungal perspective, both pathogenic strains possess a much larger repertoire of genes involved in the degradation of plant structural compounds. Moreover, plant-pathogenic *F. oxysporum* strains but not endophytic strains contain Secreted in Xylem (SIX) effectors that can be detected in the xylem sap proteome of infected plants, and it has been shown that these effectors play important roles in the devel-

opment of disease symptoms, by largely unknown mechanisms (Gawehns et al. 2015; Jangir et al. 2021). This evidence further underpins the importance of these xylem-localized interactions and distinctions between pathogen and endophyte.

Lastly, we only observed damaged cells among pathogen Fo5176- and Fo4287-infected plant roots (Supplementary Fig. S7A), using a trypan blue staining method to discriminate viable cells from cells with damaged membranes (Altman et al. 1993), although none of the colonized or infected plants showed H<sub>2</sub>O<sub>2</sub> accumulation around the interaction sites with fungal hyphae (Supplementary Fig. S7B). One explanation for the absence of the reactive oxygen species (ROS) is the presence of oxidative burst inhibitory effectors, such catalase, peroxidase, and reductase (Hemetsberger et al. 2012; Marroquin-Guzman et al. 2017; Molina and Kahmann 2007), which are present in pathogenic and endophytic F. oxysporum strains (L.-J. Ma unpublished data). The other possibility is that ROS burst was induced within minutes to a few hours postinoculation (de Lamo and Takken 2020; Humbert et al. 2015) and our observation may have missed this critical time window.

Plants and microbes may establish beneficial, neutral, or antagonistic relationships. Our results introduced a focal point of one or both the host vasculature and its surrounding tissues at the PMZ, where the molecular battle differentiating endophytes versus pathogens is likely to take place. From the fungal evolutionary perspective, this study draws attention to differential nutrient acquisition within hosts (e.g., amino acids, nitrogen sources) as well as to the differential secretion of effectors that interfere in host immunity and induce differential deposition of structural components, such as callose and lignin, to have distinct colonization levels within the xylem. Collectively, this work added

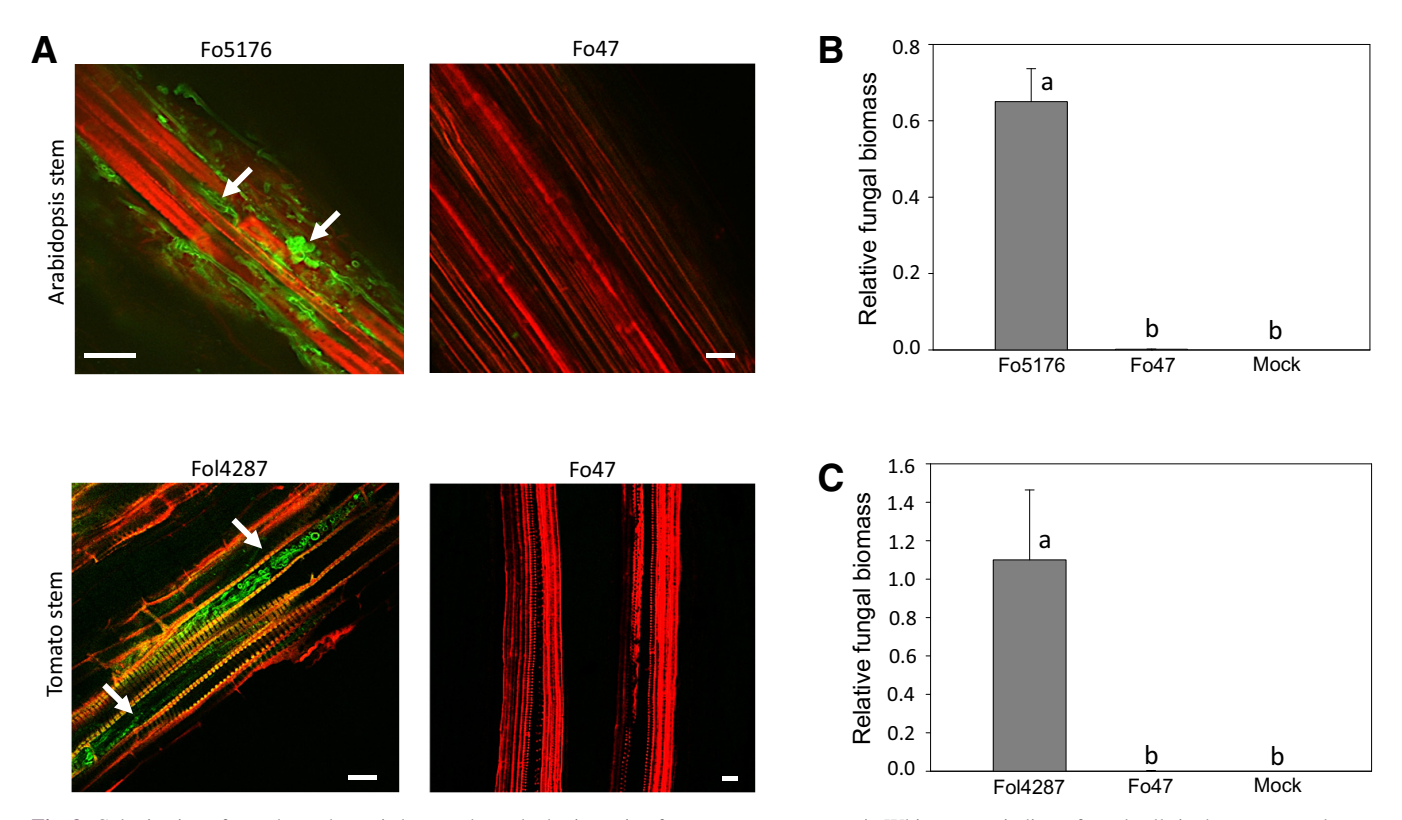


Fig. 3. Colonization of stem by pathogenic but not the endophytic strain of *Fusarium oxysporum*. A, White arrows indicate fungal cells in the stem vasculature of plants inoculated with the pathogenic strains of *F. oxysporum*. Notice the absence of fungal cells in the stems of plants inoculated with the endophytic strain Fo47. Scale bar = 50 µm. B, Relative fungal biomass by quantitative PCR (qPCR) in stems of *Arabidopsis thaliana* plants inoculated with Fo5176 or Fo47 at 16 days postinoculation (dpi). C, Relative fungal biomass by qPCR in stems of tomato plants inoculated with Fol4287 or Fo47 at 16 dpi. Genomic DNA was extracted from the stems of inoculated plants and was used for relative fungal biomass determination for qPCR. Error bars indicate standard error. Different letters in B and C denote significant differences (analysis of variance, Tukey).

to our understanding of the differential interactions between a *Fusarium* endophyte and *Fusarium* pathogens with plant hosts.

The researchers used endophyte strain *F. oxysporum* Fo47 and the plant pathogens Fo5176 and Fo14287 in this study. The strains were stored in 50% glycerol at  $-80^{\circ}$ C for long-term maintenance, were recovered onto potato dextrose agar media, then were inoculated in liquid NO<sub>3</sub>-based medium (per milliliter, 1.7 mg of yeast nitrogen base, 30 mg of sucrose, and 10.1 mg of KNO<sub>3</sub>). Liquid media suspensions were incubated under shak-

ing conditions (200 rpm) at 28°C for 5 days. The microconidia were collected using a Miracloth filter, were recovered, and were washed three times with sterile distilled water (SDW) by centrifugation at  $4,000 \times g$  for 10 min. Finally, spore concentration was determined with a hemocytometer and was diluted to  $10^6$  spores per milliliter before plant inoculation.

Seeds of *Arabidopsis thaliana* Columbia-0 and *Solanum lycopersicum* cv. M82 were propagated as follows. These seeds were maintained in darkness at 4°C for 3 days, sterilized in 70%

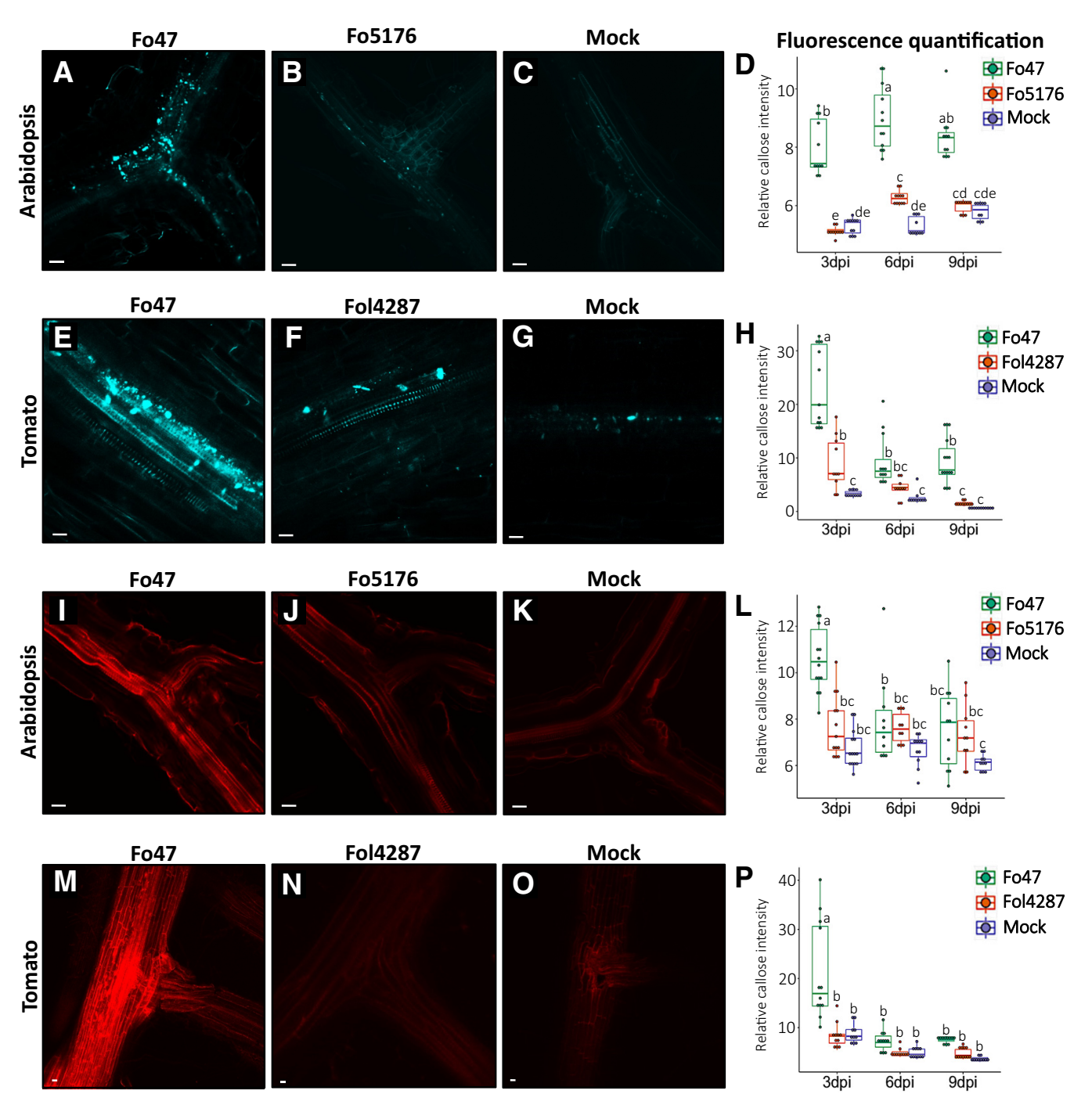


Fig. 4. Callose and lignin deposition in roots of plants colonized or infected by *Fusarium oxysporum*. **A**, *Arabidopsis* roots inoculated with Fo47, **B**, Fo5176, and **C**, mock-inoculated. **E**, Tomato roots inoculated with Fo47, **F**, Fol4287 and **G**, mock-inoculated. **D** and **H**, Callose quantification in *Arabidopsis* and tomato roots, respectively. In A and E, high blue fluorescence of aniline blue indicates high callose deposition in vessel cells of colonized roots by Fo47. **I**, *Arabidopsis* roots inoculated with Fo47, **J**, Fo5176, and **K**, mock-inoculated. **M**, Tomato roots inoculated with Fo47, **N**, Fol4287 and **O**, mock-inoculated. **L** and **P**, Lignin quantification in *Arabidopsis* and tomato roots respectively. In I and M, high red fluorescence of basic fuchsin indicates high lignin deposition mostly in the primary and lateral root junctions of plants colonized by Fo47. The microscopy photographs are representative images of roots colonized by the endophyte or infected by the pathogens at 3 days postinoculation (dpi). Scale bar = 20 μm. Different letters in D, H, L and P denote significant differences (analysis of variance, Tukey).

(vol/vol) ethanol (5 min), followed by 20% NaClO (5 min), and were then rinsed with SDW (four times) before being planted into pots with autoclaved soil-less growing media (Promix BX). Plants were grown under standard greenhouse conditions in a controlled environment growth chamber at 24°C, with photoperiods of 14 h of light and 10 h of dark. The soil was gently removed from Arabidopsis and tomato roots when they were 8 and 10 days old, respectively, using distilled water and SDW to avoid root tissue damage. Fungal inoculation followed the rootdipping protocol described by Di Pietro and Roncero (1998), with some modifications. The washed roots were dipped in the respective endophytic or pathogenic Fusarium spore suspension or SDW as mock-infection for 45 min, then, the inoculated plants were gently transplanted in fresh sterile soil medium and were maintained in a controlled environment growth chamber at 28°C, with photoperiods of 14 h of light and 10 h of dark. The experiments were carried out six times with at least 10 tomato plants and 20 Arabidopsis plants per treatment in each repetition.

The staining methods that were followed for fungal visualization were previously described by Ghareeb et al. (2011). The infected roots were soaked in ethanol overnight, were rinsed with SDW, and were incubated in 10% KOH for 12 h. After washing with SDW again, roots were incubated for 30 min (including three intervals of 2 min on vacuum conditions) in a staining solution containing 10 mg of WGA-Alexa Fluor 488 per milliliter, 20 mg of propidium iodide per milliliter, and 0.02% Tween 20 in phosphate-buffered saline, pH 7.4. The samples were observed under an Olympus FluoView FV1000 confocal microscope (Tokyo and were photographed with a Hamamatsu camera (Hamamatsu, Japan). Following the manufacturer suggestions, WGA-Alexa Fluor 488 was detected with excitation at 488 nm and emission at 500 to 540 nm (staining the fungal structures green), while propidium iodide was detected with excitation at 561 nm and emission at 580 to 660 nm (staining the plant tissues red). Moreover, 1-cm pieces of the infected stem were embedded in 5.4% agarose, were cut into thin slices with a Leica VT1000S vibratome (Wetzlar, Gemany), according to Pradhan-Mitra and Loqué (2014), were then stained, and finally, were observed as described above. For visualization of structures of RFP-tagged Fo47, the infected plant tissues were observed directly under the confocal microscope, using the RFP channel (excitation at 555 nm and emission at 584 nm).

Callose visualization was performed according to the method described by Zhang et al. (2015), with some adaptations. Colonized/infected roots were cleaned in 95% ethanol for 30 min, were incubated in an emulsifiable solution (phenol, glycerol, lactic acid, water, and ethanol at 1:1:1:18 concentration) at 65°C for 1 h, were washed with 50% ethanol and SDW, and were then stained by soaking in 0.1% aniline blue for 1 h. Callose deposition stained by aniline blue was analyzed with excitation at 395 nm and emission at 495 nm under Olympus FluoView FV1000 confocal microscope.

Visualization of lignin and suberin was performed according to the protocol described by Kurihara et al. (2015), with some modifications made by the N. Geldner research group from the University of Lausanne, Switzerland. Colonized or infected roots were fixed with 4% paraformaldehyde in phosphate-buffered saline (PBS) for 1 h at room temperature in vacuum conditions, were then washed twice for 1 min with PBS, and were transferred to ClearSee solution (10% xylitol, 15% sodium deoxycholate, 25% urea, and SDW to the final volume) at room temperature with gentle agitation for 4 days. Colonized or infected roots were stained by soaking in different staining solutions. All staining solutions were prepared in ClearSee solution, and that same solution was used for all washed steps. All samples were analyzed under the confocal microscope and camara described above. Lignin was stained with 0.2% basic fuchsin

overnight, was rinsed and washed for 30 min, and was washed again overnight. Basic fuchsin was observed with excitation at 561 nm and emission at 600 to 650 nm. Suberin was stained 0.5% auramine O for 16 h, was rinsed and washed for 30 min, and was washed again for 2 h. Auramine O was analyzed at 488 nm excitation and 505 to 530 nm emission.

Callose and lignin quantification were processed and analyzed using ImageJ software, according to Xu et al. (2020). Callose deposition was observed only in vessel cells and around the vascular cells, which facilitated its measurement using photographs with a black background to eliminate possible autofluorescence. Lignin deposition was measured focusing only on the junctions of the primary and secondary roots, sites where the lignin deposition was observed, using photographs with a black background. Average callose measurements were based on at least 10 photographs from different roots. Data were analyzed by analysis of variance (ANOVA) and Tukey's range test (P < 0.05) to compare the means among the different treatments. The Statistic 8.0 program was used for the statistical analyses.

For visualization and analysis of cell damage, colonized or infected roots were submerged for 3 to 5 min in 0.4% trypan blue solution with 0.81% NaCl and 0.06% dibasic potassium phosphate and were washed twice with PBS, according to the methodology described by Altman et al. (1993). The observation of H<sub>2</sub>O<sub>2</sub> production was performed using the protocol described by Molina and Kahmann (2007). Colonized or infected roots were dipped in 1-mg/ml diaminobenzedene solution for 1 h in darkness at room temperature, then were washed with PBS once. Cell damage and H<sub>2</sub>O<sub>2</sub> were observed under the light microscope Nikon Eclipse E200 (Tokyo) and were photographed with a Pixelink camera (Ontario, Canada).

To confirm the presence of Fo47 in the root tissues of Arabidopsis and tomato plants, the fungus was re-isolated from the roots of plants after 8, 16, and 25 dpi, using the protocol described by Elmer et al. (1994), with some modifications. The entire plants were removed from the soil and were washed first under tap water, then with abundant SDW, to remove the soil particles. Under the laminar flow hood, roots were dipped in 10% NaClO for 1 min, were washed several times with SDW, and were blotted dry, using Kimwipe paper towels. Small plant tissue pieces were placed on a solid Komada Fusarium-selective medium (Komada 1975) and were incubated at 28°C. After 2 to 3 days, the fungal colonies were transferred to new Petri dishes with Komada medium and were used for single-spore isolation. Using the Qiagen plant DNA extraction kit (Hilden, Germany), DNA of three different fungal colonies isolated from Arabidopsis and tomato plants was collected. Fo47 strain-specific effector genes FOZG\_17267 (jgi|FusoxFo47\_2|262755), FOZG\_10369 (jgi|FusoxFo47\_2|239495), and FOZG\_17668 (jgi|FusoxFo47\_2|276745) were used to design primers for strain-specific PCR amplification and sequencing as follows: Fo47\_262755 F: CTACCAGGAAGCCTAGGCCGT C; R: CATAGACCAACCACGGCCCAGG; Fo47\_239495 F: CTTCAACAACGCCATTGTCGCC; R: CTGAGGGCATTGT TGGCTGACC; Fo47\_276745 F: CACCAGGACAATCTTATC ACAC; R: GAGCGCCCCTAAGGACGATGCG. PCR products were sequenced by Genewiz Inc. (Cambridge, MA, U.S.A.), and the sequences were analyzed by BLAST in Joint Genome Institute (JGI) Genome Portal, FungiDB, and the National Center for Biotechnology Information (NCBI).

For detection of the pathogenic Fol4287 and Fo5175 as well as the endophytic Fo47 from above-ground tissues, the stems of 10 tomato and 50 *Arabidopsis* plants were harvested after 16 dpi. For genomic DNA extraction, stem material was frozen in liquid nitrogen, was ground to powder, and was extracted, using the Qiagen plant DNA extraction kit described above. The reverse transcription-qPCR analysis was

performed using a Mastercycler (Eppendorf), following the manufacturer instructions of the SYBR Green PCR master mix kit (Applied Biosystems). F. oxysporums strains were detected with primers Actin-fw (5'-GCACGATGTTGCTGTAGAGAG-3') and Actin-re (5'-GATTGGCGCGGAACGCTTTAG-3'), amplifying a conserved region of the actin gene. Arabidopsis pentatricopeptide repeat was amplified with primers Pent-fw (5'-GAGGATGATTCACCCCAACGAAG-3'), Pent-re (5'- CC TCACTAATGTGTCCATCAATC-3'), and tomato beta-tubulin served as reference genes for normalization, amplified with primers Tubulin-fw (5'-GATTTGCCCACTAACCTCTCGT-3') and Tubulin-re (5'- ACCTCCTTTGTGCTCATCTTACCC-3'). Relative amounts of fungal DNA were calculated relative to the amount of pentatricopeptide repeat (for A. thaliana) and betatubulin (for tomato) DNA respectively, using the cycle threshold  $2^{-\Delta\Delta Ct}$  method (Livak and Schmittgen 2001). Three biological replicates with three repetitions in each one was analyzed, and significant differences were determined (ANOVA, Tukey).

The proteomes of Fo47 (Wang et al. 2020), Fo5176 (Fokkens et al. 2020), and Fol4287 (Ayhan et al. 2018; Ma et al. 2010) were downloaded from the JGI MycoCosm portal (Grigoriev et al. 2012). SignalP 5.0 (Almagro-Armenteros et al. 2019) was used to identify putative secreted proteins. These proteins were analyzed with OrthoFinder 2.5.4 (Emms and Kelly 2019) for orthogroups determination. Finally, protein annotation was performed using InterProScan 5.38-76.0 (Jones et al. 2014). Annotations of proteins involved in plant compound degradation were then manually extracted.

*Arabidopsis* genes involved in callose biosynthesis were previously described by Ellinger and Voigt 2014. Genes involved in the regulation of lignin deposition were identified from information reported by Liu et al. (2018) and Vanholme et al. (2010).

The RNA-seq dataset was previously described and deposited in the NCBI Short Read Archive with accession number GSE87352. In short, reads were mapped to reference genomes of *Arabidopsis* (annotation version Araport11 [Cheng et al. 2017]), Fo5176 (Fokkens et al. 2020), and Fo47 (Wang et al. 2020), using HISAT2 version 2.0.5 (Kim et al. 2015). Mapped reads were used to quantify the transcriptome by StringTie version 1.3.4 (Pertea et al. 2015). Read count normalization was conducted using DESeq2 version 1.27.32 (Love et al. 2014). Researchers first averaged normalized read counts per condition and were then transformed by log<sub>2</sub> (normalized read count + 1) and Z-scaled, and were then visualized in ggplot2 version 3.3.0 and pheatmap (version 1.0.12).

## **Acknowledgments**

We appreciate D. Tieman at University of Florida and Tomato Genetics Resource Center (TGRC) for making available seeds of *Solanum lycopersicum* cv. M82; J. Manners and D. Gardiner of CSIRO for providing strain Fo5176; C. Joyner and D. O'Neil of the College of Natural Sciences Greenhouse at University of Massachusetts (UMASS) and UMASS undergraduate students M. Rodrigues, S. Andersen, and H. Lynch for their support with some of the experiments conducted in the greenhouse.

## **Literature Cited**

- Aimé, S., Alabouvette, C., Steinberg, C., and Olivain, C. 2013. The endophytic strain *Fusarium oxysporum* Fo47: A good candidate for priming the defense responses in tomato roots. Mol. Plant-Microbe Interact. 26:918-926.
- Akhter, A., Hage-Ahmed, K., Soja, G., and Steinkellner, S. 2016. Potential of *Fusarium* wilt-inducing chlamydospores, in vitro behaviour in root exudates and physiology of tomato in biochar and compost amended soil. Plant Soil 406:425-440.
- Alabouvette, C. 1986. Fusarium-wilt suppressive soils from the Châteaurenard region: Review of a 10-year study. Agronomie 6:273-284.
- Almagro-Armenteros, J. J., Tsirigos, K. D., Sønderby, C. K., Petersen, T. N., Winther, O., Brunak, S., von Heijne, G., and Nielsen, H. 2019. SignalP

- 5.0 improves signal peptide predictions using deep neural networks. Nat. Biotechnol. 37:420-423.
- Altman, S. A., Banders, L., and Bao, G. 1993. Comparison of trypan blue dye exclusion and fluorometric assays for mammalian cell viability determinations. Biotechnol. Progr. 9:671-674.
- Araujo, L., Bispo, W. M. S., Cacique, I. S., Moreira, W. R., and Rodrigues, F. Á. 2014. Resistance in mango against infection by *Ceratocystis fim-briata*. Phytopathology 104:820-833.
- Armitage, A. D., Taylor, A., Sobczyk, M. K., Baxter, L., Greenfield, B. P. J., Bates, H. J., Wilson, F., Jackson, A. C., Ott, S., Harrison, R. J., and Clarkson, J. P. 2018. Characterisation of pathogen-specific regions and novel effector candidates in *Fusarium oxysporum* f. sp. cepae. Sci. Rep. 8:13530.
- Ayhan, D. H., López-Díaz, C., Di Pietro, A., and Ma, L. J. 2018. Improved assembly of reference genome *Fusarium oxysporum* f. sp. *lycopersici* strain Fol4287. Microbiol. Resource Announc. 7:e00910-18.
- Bao, J., Fravel, D., Lazarovits, G., Chellemi, D., van Berkum, P., and O'Neill, N. 2004. Biocontrol genotypes of *Fusarium oxysporum* from tomato fields in Florida. Phytoparasitica 32:9-20.
- Benhamou, N., and Garand, C. 2001. Cytological analysis of defense-related mechanisms induced in pea root tissues in response to colonization by nonpathogenic Fusarium oxysporum Fo47. Phytopathology 91:730-740.
- Benhamou, N., Garand, C., and Goulet, A. 2002. Ability of nonpathogenic Fusarium oxysporum strain Fo47 to induce resistance against Pythium ultimum infection in cucumber. Appl. Environ. Microbiol. 68:4044-4060.
- Bhuiyan, N. H., Selvaraj, G., Wei, Y., and King, J. 2009. Role of lignification in plant defense. Plant Signal. Behav. 4:158-159.
- Bishop, C. D., and Cooper, R. M. 1983. An ultrastructural study of root invasion in three vascular wilt diseases. Physiol. Plant Pathol. 22:15-IN13.
- Brader, G., Compant, S., Vescio, K., Mitter, B., Trognitz, F., Ma, L. J., and Sessitsch, A. 2017. Ecology and genomic insights into plant-pathogenic and plant-nonpathogenic endophytes. Ann. Rev. Phytopathol. 55:61-83.
- Cajero-Sánchez, W., García-Ponce, B., Sánchez, M. P., Álvarez-Buylla, E. R., and Garay-Arroyo, A. 2017. Identifying the transition to the maturation zone in three ecotypes of *Arabidopsis thaliana* roots. Commun. Integr. Biol. 11:e1395993.
- Cal, A. D., Pascual, S., and Melgarejo, P. 1997. Infectivity of chlamydospores vs microconidia of *Fusarium oxysporum* f.sp. *lycopersici* on tomato. J. Phytopathol. 145:231-233.
- Cheng, C.-Y., Krishnakumar, V., Chan, A. P., Thibaud-Nissen, F., Schobel, S., and Town, C. D. 2017. Araport11: A complete reannotation of the *Arabidopsis thaliana* reference genome. Plant J. 89:789-804.
- Dean, R., Van Kan, J. A. L., Pretorius, Z. A., Hammond-Kosack, K. E., Di Pietro, A., Spanu, P. D., Rudd, J. J., Dickman, M., Kahmann, R., Ellis, J., and Foster, G. D. 2012. The top 10 fungal pathogens in molecular plant pathology. Mol. Plant Pathol. 13:414-430.
- de Lamo, F. J., and Takken, F. L. W. 2020. Biocontrol by Fusarium oxysporum using endophyte-mediated resistance. Front. Plant Sci. 11:37.
- Delulio, G. A., Guo, L., Zhang, Y., Goldberg, J. M., Kistler, H. C., and Ma, L. J. 2018. Kinome expansion in the *Fusarium oxysporum* species complex driven by accessory chromosomes. mSphere 3:e00231-18.
- Demers, J. E., Gugino, B. K., and Jiménez-Gasco, M. M. 2015. Highly diverse endophytic and soil *Fusarium oxysporum* populations associated with field-grown tomato plants. Appl. Environ. Microbiol. 81:81-90.
- Di Pietro, A., and Roncero, M. I. 1998. Cloning, expression, and role in pathogenicity of pg1 encoding the major extracellular endopolygalacturonase of the vascular wilt pathogen *Fusarium oxysporum*. Mol. Plant-Microbe Interact. 11:91-98.
- Dong, S., Raffaele, S., and Kamoun, S. 2015. The two-speed genomes of filamentous pathogens: Waltz with plants. Curr. Opin. Genet. Dev. 35: 57.65
- Ellinger, D., and Voigt, C. 2014. Callose biosynthesis in Arabidopsis with a focus on pathogen response: What we have learned within the last decade. Ann. Bot. 114:1349-1358.
- Elmer, W. H., Wick, R. L., and Aviland, P. H. 1994. Vegetative compatibility among Fusarium oxysporum f. sp. basilicum isolates recovered from basil seed and infected plants. Plant Dis. 78:789-791.
- Emms, D. M., and Kelly, S. 2019. OrthoFinder: Phylogenetic orthology inference for comparative genomics. Genome Biol. 20:238.
- Fokkens, L., Guo, L., Dora, S., Wang, B., Ye, K., Sánchez-Rodríguez, C., and Croll, D. A. 2020. Chromosome-scale genome assembly for the *Fusar-ium oxysporum* strain Fo5176 to establish a model *Arabidopsis*-fungal pathosystem. G3 Genes Genom. Genet. 10:3549-3555.
- Galazka, J. M., and Freitag, M. 2014. Variability of chromosome structure in pathogenic fungi of 'ends and odds'. Curr. Opin. Microbiol. 20:19-26.
- Gawehns, F., Ma, L., Bruning, O., Houterman, P. M., Boeren, S., Cornelissen, B. J. C., Rep, M., and Takken, F. L. W. 2015. The effector repertoire

- of *Fusarium oxysporum* determines the tomato xylem proteome composition following infection. Front. Plant Sci. 6:967.
- Ghareeb, H., Becker, A., Iven, T., Feussner, I., and Schirawski, J. 2011. Sporisorium reilianum infection changes inflorescence and branching architectures of maize. Plant Physiol. 156:2037-2052.
- Gordon, T. R. 2017. *Fusarium oxysporum* and the Fusarium Wilt Syndrome. Annu. Rev. Phytopathol. 55:23-39.
- Graca, J. 2015. Suberin: The biopolyester at the frontier of plants. Front. Chem. 3:62.
- Grigoriev, I. V., Nordberg, H., Shabalov, I., Aerts, A., Cantor, M., Goodstein,
  D., Kuo, A., Minovitsky, S., Nikitin, R., Ohm, R. A., Otillar, R., Poliakov,
  A., Ratnere, I., Riley, R., Smirnova, T., Rokhsar, D., and Dubchak, I. 2012.
  The genome portal of the Department of Energy Joint Genome Institute.
  Nucleic Acids Res. 40:D26-D32.
- Guo, L., Yu, H., Wang, B., Vescio, K., DeIulio, G. A., Yang, H., Berg, A., Zhang, L., Edel-Hermann, V., Steinberg, C., Kistler, H. C., and Ma, L.-J. 2021. Metatranscriptomic comparison of endophytic and pathogenic Fusarium-Arabidopsis interactions reveals plant transcriptional plasticity. Mol. Plant-Microbe Interact. 34:1071-1083.
- Halpern, H. C., Bell, A. A., Wagner, T. A., Liu, J., Nichols, R. L., Olvey, J., Woodward, J. E., Sanogo, S., Jones, C. A., Chan, C. T., and Brewer, M. T. 2018. First report of *Fusarium* wilt of cotton caused by *Fusarium oxysporum* f. sp. vasinfectum race 4 in Texas, U.S.A. Plant Dis. 102:446.
- Hane, J. K., Rouxel, T., Howlett, B. J., Kema, G. H., Goodwin, S. B., and Oliver, R. P. 2011. A novel mode of chromosomal evolution peculiar to filamentous Ascomycete fungi. Genome Biol. 12:R45.
- Hemetsberger, C., Herrberger, C., Zechmann, B., Hillmer, M., and Doehlemann, G. 2012. The *Ustilago maydis* effector Pep1 suppresses plant immunity by inhibition of host peroxidase activity. PLoS Pathog. 8:e1002684.
- Houterman, P. M., Speijer, D., Dekker, H. L., DE Koster, C. G., Cornelissen, B. J., and Rep, M. 2007. The mixed xylem sap proteome of *Fusarium oxysporum*-infected tomato plants. Mol. Plant Pathol. 8:215-221.
- Hückelhoven, R. 2007. Cell wall-associated mechanisms of disease resistance and susceptibility. Annu. Rev. Phytopathol 45:101-127.
- Humbert, C., Aimé, S., Alabouvette, C., Steinberg, C., and Olivain, C. 2015. Remodelling of actin cytoskeleton in tomato cells in response to inoculation with a biocontrol strain of *Fusarium oxysporum* in comparison to a pathogenic strain. Plant Pathol. 64:1366-1374.
- Iriti, M., and Faoro, F. 2009. Chitosan as a MAMP, searching for a PRR. Plant Signal. Behav. 4:66-68.
- Jangir, P., Mehra, N., Sharma, K., Singh, N., Rani, M., and Kapoor, R. 2021. Secreted in xylem genes: Drivers of host adaptation in *Fusarium oxysporum*. Front. Plant Sci. 12:628611.
- Jones, P., Binns, D., Chang, H.-Y., Fraser, M., Li, W., McAnulla, C., McWilliam, H., Maslen, J., Mitchell, A., Nuka, G., Pesseat, S., Quinn, A. F., Sangrador-Vegas, A., Scheremetjew, M., Yong, S. Y., Lopez, R., and Hunter, S. 2014. InterProScan 5: Genome-scale protein function classification. Bioinformatics 30:1236-1240.
- Kim, D., Langmead, B., and Salzberg, S. L. 2015. HISAT: A fast spliced aligner with low memory requirements. Nat. Methods 12:357-360.
- Kistler, H. C. 1997. Genetic diversity in the plant-pathogenic fungus Fusarium oxysporum. Phytopathology 87:474-479.
- Komada, H. 1975. Development of a selective medium for quantitative isolation of *Fusarium oxysporum* from natural soil. Rev. Plant. Prot. Res. 8:114-125.
- Kondo, Y., Tamaki, T., and Fukuda, H. 2014. Regulation of xylem cell fate. Front. Plant Sci. 5:315.
- Kurihara, D., Mizuta, Y., Sato, Y., and Higashiyama, T. 2015. ClearSee: A rapid optical clearing reagent for whole-plant fluorescence imaging. Development 142:4168-4179.
- Lagopodi, A. L., Ram, A. F., Lamers, G. E., Punt, P. J., Van den Hondel, C. A., Lugtenberg, B. J., and Bloemberg, G. V. 2002. Novel aspects of tomato root colonization and infection by *Fusarium oxysporum* f. sp. *radicis-lycopersici* revealed by confocal laser scanning microscopic analysis using the green fluorescent protein as a marker. Mol. Plant-Microbe Interact. 15:172-179.
- Lee, M. H., Jeon, H. S., Kim, S. H., Chung, J. H., Roppolo, D., Lee, H. J., Cho, H. J., Tobimatsu, Y., Ralph, J., and Park, O. K. 2019. Lignin-based barrier restricts pathogens to the infection site and confers resistance in plants. EMBO J. 38:e101948.
- Li, C., Yang, J., Li, W., Sun, J., and Peng, M. 2017. Direct root penetration and rhizome vascular colonization by *Fusarium oxysporum* f. sp. *cubense* are the key steps in the successful infection of Brazil Cavendish. Plant Dis. 101:2073-2078.
- Liu, Q., Luo, L., and Zheng, L. 2018. Lignins: Biosynthesis and biological functions in plants. Int. J. Mol. Sci. 19:335.

- Livak, K. J., and Schmittgen, T. D. 2001. Analysis of relative gene expression data using real-time quantitative PCR and the  $2^{-\Delta\Delta}$  C(T) method. Methods 25:402-408
- Love, M. I., Huber, W., and Anders, S. 2014. Moderated estimation of fold change and dispersion for RNA-seq data with DESeq2. Genome Biol. 15:550.
- Ma, L. J., Geiser, D. M., Proctor, R. H., Rooney, A. P., O'Donnell, K., Trail, F., Gardiner, D. M., Manners, J. M., and Kazan, K. 2013. Fusarium pathogenomics. Annu. Rev. Microbiol. 67:399-416.
- Ma, L. J., van der Does, H. C., Borkovich, K. A., Coleman, J. J., Daboussi, M. J., Di Pietro, A., Dufresne, M., Freitag, M., Grabherr, M., Henrissat, B., Houterman, P. M., Kang, S., Shim, W. B., Woloshuk, C., Xie, X., Xu, J. R., Antoniw, J., Baker, S. E., Bluhm, B. H., Breakspear, A., Brown, D. W., Butchko, R. A., Chapman, S., Coulson, R., Coutinho, P. M., Danchin, E. G., Diener, A., Gale, L. R., Gardiner, D. M., Goff, S., Hammond-Kosack, K. E., Hilburn, K., Hua-Van, A., Jonkers, W., Kazan, K., Kodira, C. D., Koehrsen, M., Kumar, L., Lee, Y. H., Li, L., Manners, J. M., Miranda-Saavedra, D., Mukherjee, M., Park, G., Park, J., Park, S. Y., Proctor, R. H., Regev, A., Ruiz-Roldan, M. C., Sain, D., Sakthikumar, S., Sykes, S., Schwartz, D. C., Turgeon, B. G., Wapinski, I., Yoder, O., Young, S., Zeng, Q., Zhou, S., Galagan, J., Cuomo, C. A., Kistler, H. C., and Rep, M. 2010. Comparative genomics reveals mobile pathogenicity chromosomes in Fusarium. Nature 464:367-373.
- Marroquin-Guzman, M., Hartline, D., Wright, J. D., Elowsky, C., Bourret, T. J., and Wilson, R. A. 2017. The *Magnaporthe oryzae* nitrooxidative stress response suppresses rice innate immunity during blast disease. Nature Microbiol. 2:17054.
- Michielse, C. B., and Rep, M. 2009. Pathogen profile update: *Fusarium oxysporum*. Mol. Plant Pathol. 10:311-324.
- Molina, L., and Kahmann, R. 2007. An *Ustilago maydis* gene involved in H<sub>2</sub>O<sub>2</sub> detoxification is required for virulence. Plant Cell 19:2293-2309.
- Olivain, C., Humbert, C., Nahalkova, J., Fatehi, J., L'Haridon, F., and Alabouvette, C. 2006. Colonization of tomato root by pathogenic and nonpathogenic *Fusarium oxysporum* strains inoculated together and separately into the soil. Appl. Environ. Microbiol. 72:1523-1531.
- Olivain, C., Trouvelot, S., Binet, M.-N., Cordier, C., Pugin, A., and Alabouvette, C. 2003. Colonization of flax roots and early physiological responses of flax cells inoculated with pathogenic and nonpathogenic strains of *Fusarium oxysporum*. Appl. Environ. Microbiol. 69:5453-5462.
- Pegg, G. F. 1976. The response of ethylene-treated tomato plants to infection by Verticillium albo-atrum. Physiol. Plant Pathol. 9:215-226.
- Pertea, M., Pertea, G. M., Antonescu, C. M., Chang, T.-C., Mendell, J. T., and Salzberg, S. L. 2015. StringTie enables improved reconstruction of a transcriptome from RNA-seq reads. Nat. Biotechnol. 33:290-295.
- Pradhan Mitra, P., and Loqué, D. 2014. Histochemical staining of Arabidopsis thaliana secondary cell wall elements. J. Vis. Exp. 87:51381.
- Pu, X., Xie, B., Li, P., Mao, Z., Ling, J., Shen, H., Zhang, J., Huang, N., and Lin, B. 2014. Analysis of the defence-related mechanism in cucumber seedlings in relation to root colonization by nonpathogenic *Fusarium* oxysporum CS-20. FEMS Microbiol. Lett. 355:142-151.
- Rahman, M. Z., Ahmad, K., Siddiqui, Y., Saad, N., Hun, T. G., Mohd Hata, E., Rashed, O., Hossain, M. I., and Kutawa, A. B. 2021. First report of Fusarium wilt disease on watermelon caused by Fusarium oxysporum f. sp. niveum (FON) in Malaysia. Plant Dis. 105:4169.
- Redkar, A., Sabale, M., Schudoma, C., Zechmann, B., Gupta, Y. K., López-Berges, M. S., Venturini, G., Gimenez-Ibanez, S., Turrà, D., Solano, R., and Di Pietro, A. 2022. Conserved secreted effectors contribute to endophytic growth and multihost plant compatibility in a vascular wilt fungus. Plant Cell 34:3214-3232.
- Rep, M., van der Does, H. C., Meijer, M., van Wijk, R., Houterman, P. M., Dekker, H. L., de Koster, C. G., and Cornelissen, B. J. 2004. A small, cysteine-rich protein secreted by *Fusarium oxysporum* during colonization of xylem vessels is required for I-3-mediated resistance in tomato. Mol. Microbiol. 53:1373-1383.
- Somssich, M., Khan, G. A., and Persson, S. 2016. Cell wall heterogeneity in root development of *Arabidopsis*. Front Plant Sci. 07:1242.
- van Dam, P., Fokkens, L., Schmidt, S. M., Linmans, J. H. J., Kistler, H. C., Ma, L. J., and Rep, M. 2016. Effector profiles distinguish formae speciales of Fusarium oxysporum. Environ. Microbiol. 18:4087-4102.
- Vanholme, R., Demedts, B., Morreel, K., Ralph, J., and Boerjan, W. 2010. Lignin biosynthesis and structure. Plant Physiol. 153:895-905.
- Veloso, J., and Díaz, J. 2012. Fusarium oxysporum Fo47 confers protection to pepper plants against Verticillium dahliae and Phytophthora capsici, and induces the expression of defence genes. Plant Pathol. 61:281-288.
- Viljoen, A., Mostert, D., Chiconela, T., Beukes, I., Fraser, C., Dwyer, J., Murray, H., Amisse, J., Matabuana, E. L., Tazan, G., Amugoli, O. M., Mondjana, A., Vaz, A., Pretorius, A., Bothma, S., Rose, L. J., Beed, F., Dusunceli, F., Chao, C. -. P., and Molina, A. B. 2020. Occurrence and

- spread of the banana fungus  $Fusarium\ oxysporum\ f.\ sp.\ cubense\ TR4$  in Mozambique. S. Afr. J. Sci. 116:1-11.
- Vlaardingerbroek, I., Beerens, B., Rose, L., Fokkens, L., Cornelissen, B. J. C., and Rep, M. 2016. Exchange of core chromosomes and horizontal transfer of lineage-specific chromosomes in *Fusarium oxysporum*. Environ. Microbiol. 18:3702-3713.
- Wang, B., Yu, H., Jia, Y., Dong, Q., Steinberg, C., Alabouvette, C., Edel-Hermann, V., Kistler, H. C., Ye, K., Ma, L. J., and Guo, L. 2020. Chromosome-scale genome assembly of *Fusarium oxysporum* strain Fo47, a fungal endophyte and biocontrol agent. Mol. Plant-Microbe Interact. 33:1108-1111.
- Williams, A. H., Sharma, M., Thatcher, L. F., Azam, S., Hane, J. K., Sperschneider, J., Kidd, B. N., Anderson, J. P., Ghosh, R., Garg, G., Lichtenzveig, J., Kistler, H. C., Shea, T., Young, S., Buck, S.-A. G., Kamphuis, L. G., Saxena, R., Pande, S., Ma, L. J., Varshney, R. K., and Singh, K. B. 2016. Comparative genomics and prediction of conditionally dispensable sequences in legume–infecting *Fusarium oxysporum formae*

- speciales facilitates identification of candidate effectors. BMC Genomics 17:191.
- Xu, Y., Zhang, J., Shao, J., Feng, H., Zhang, R., and Shen, Q. 2020. Extracellular proteins of *Trichoderma guizhouense* elicit an immune response in maize (*Zea mays*) plants. Plant Soil 449:133-149.
- Yang, H., Yu, H., and Ma, L. J. 2020. Accessory chromosomes in *Fusarium oxysporum*. Phytopathology 110:1488-1496.
- Yu, H., Ayhan, D. H., Diener, A. C., and Ma, L. J. 2020. Genome sequence of *Fusarium oxysporum* f. sp. *matthiolae*, a Brassicaceae pathogen. Mol. Plant-Microbe Interact. 33:569-572.
- Zhang, M., Ahmed Rajput, N., Shen, D., Sun, P., Zeng, W., Liu, T., Juma Mafurah, J., and Dou, D. 2015. A *Phytophthora sojae* cytoplasmic effector mediates disease resistance and abiotic stress tolerance in *Nicotiana benthamiana*. Sci. Rep. 5:10837.
- Zhang, Y., and Ma, L. J. 2017. Deciphering pathogenicity of *Fusar-ium oxysporum* from a phylogenomics perspective. Adv. Genet. 100: 179-209.